Finite Element Analysis and Parametric Study of Electromagnetic Forming Process

Gaurish A. Walke[a*], Ashish Kulkarni[b], R. Vasudevan[a]

a. SMBS, VIT University, Vellore, Tamil Nadu, India

b. SIMULIA Indus, 3DPLM Software solutions co. ltd, Pune, Maharashtra, India

Abstract—**The desire to produce light weight structures has stimulated the automotive and aerospace industry to direct their attention towards employing light weight, high strength to weight ratio material such as aluminium alloys. This has developed interest in understanding electromagnetic forming (EMF), which produces high strain rate using induced electromagnetic fields, thus enhancing the formability of aluminium alloys and reducing its wrinkling and spring-back. To get a better insight of the behavior and physics of EMF process a numerical model is highly necessary which helps to reduce the cost and time of the analysis. In this study, a three dimensional numerical simulation of tube compression process has been carried out on aluminium alloy AA3003 using commercially available finite element tool, Abaqus®. Loosely coupled approach has been used in which the effect of tube deformation on electromagnetic field has been neglected. The final tube deformation is validated with experimental results. It was seen that there is a good correlation between the numerical simulation and the experimental results. The primary emphasis was made to determine the effect of discharge current frequency and discharge energy on final tube deformation and hence to find the optimum range of discharge current frequency and energy level of the system. The optimum discharge current frequency range was determined at different discharge energy levels. This study could serve as a valuable piece of information for better design of the EMF process by controlling the process parameters.**

Keywords—Electromagnetic forming; FEA analysis; tube compression; multiphysics; energy efficiency

I. INTRODUCTION

In electromagnetic forming (EMF) process, the magnetic pressure is developed as a result of the interaction between the transient currents of high intensity between adjacent conductors. This pressure is used for the deformation of electrically conductive metals. The magnetic field produced in the coil induces eddy currents in the nearby work piece that flows in the opposite direction to that of discharge current which causes the mutual repulsion between the work piece and the forming coil. This repulsion is large enough to deform the workpiece beyond the elastic yield strength and thus produces the permanent deformation of the work piece at very high strain rates. For better understanding the behavior and physics of EMF process a numerical model is highly necessary to reduce the cost and time of the analysis. The basic equations of the physics involved in electromagnetic forming (EMF) process are presented in [1]. References [2, 3] provided the solution of the forming

system analytically using a simpler set of electromagnetic equations. Takatsu et al[4] has provided a detailed approach to model the electromagnetic forming of thin metal workpieces, and compared their numerical results with experimental results. Modeling and computation of Lorentz forces for a stranded coil and job piece geometry are reported by [5]. The basic aspects of electromagnetic sheet metal forming process are numerically simulated by Siddiqui [6] using finite difference code to obtain the electromagnetic forces and these forces were used in axisymmetric model to get the deformation of sheet metal. Ping and Feng [7] has presented a numerical simulation of electromagnetic tube compression process using axisymmetric model. A parametric study to determine the effect of change in coil height [7] and change in current frequency on deformation of tube [8] was carried. Siddiqui has also carried out the parametric study on sheet metal forming by varying the setup geometry and other process parameters [9]. Many of the industrial processes are non-axisymmetric which are tackled by solid mesh elements that can capture wrinkling in the workpieces. It was found that 15% better results in terms of amplitude of magnetic flux density with 3D modeling could be achieved as compared to those with 2D axisymmetric simulation [10]. The influence of process and geometrical parameters were investigated analytically and experimentally by [11]. The EMF process involves high energy input and hence determining its efficiency is very needful. The discharge current frequency and the discharge energy are one of the key parameters of the EMF process which can control the efficiency of the process.

In the present study, the numerical simulation of tube compression process is carried out on 3D model and the numerical predictability of Abaqus® is determined by validating the numerical results of tube final deformation with the experimental results available in literature [7]. The basic objective of improving the system efficiency is investigated i.e. the parametric study is performed to determine the individual effect of discharge current frequency and discharge energy on the energy efficiency of the EMF process. The study can provide valuable information which could be used for designing the EMF process to obtain a better efficiency.

II. FEA OF ELECTROMAGNETIC TUBE COMPRESSION

A. *Finite element model for electromagnetic analysis*

An EMF system considered for the simulation consists of a 17 turns of a helical solenoid copper coil, concentric

with the aluminium tube and placed outside it for compression. The gap between the coil and the tube is filled with air which is assumed to have the properties of vacuum. Fig.1 depicts the schematic set up used for the numerical simulation of electromagnetic tube compression process. For numerical modeling, the experimental parameters for both tube and coil were considered from [7]. The FEA model for tube forming is shown in Fig.2. Due to symmetry of the system, the quarter model has been used for the present analysis. It is to be noted that 18000 elements and 3825 elements have been used to discretize the tube and the coil, respectively. The air region has been discretized using 130000 elements. The element type used was EMC3D8 with the degree of freedom associated as magnetic vector potential. The coil, tube and the near field region were meshed with refined mesh using structured mesh technique. 10 elements were used along the thickness of the tube 120 elements along the tube height and 12 elements along the circumference. The far field region was meshed with course mesh using sweep meshing technique.
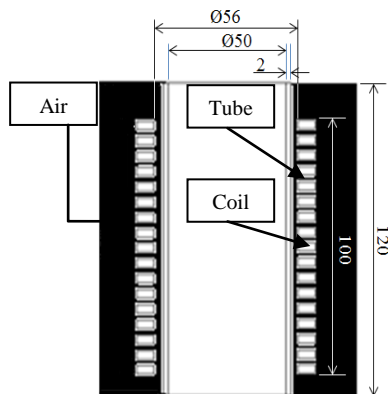

Fig. 1 Schematic of model used for electromagnetic tube compression process (All dimensions are in mm.)
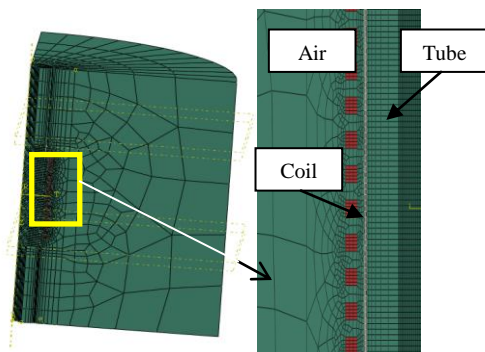

Fig. 2 Finite element model of the electromagnetic process.

B. Loads and boundary condition

The load applied during the analysis is damped sinusoidal current as given by (1). For the present analysis, the current is considered to be applied to the volume of the coil in the form of body current density.

$$I = U . \sqrt{\frac{C}{L}} . e^{(-\beta t)} . \sin(\omega t) \qquad (1)$$

where, I is discharge current in ampere, U is the initial discharge voltage, β is the current damping coefficient, ω is the discharge current frequency. The boundary conditions considered for the simulation are zero magnetic vector potential on the symmetry planes and external far field boundaries of the domain.

C. Structural model

The tube region is considered for the structural model and analysis. During the analysis the mesh was kept same as that of electromagnetic model, i.e. 120 elements along the tube height 10 elements along its thickness and 12 elements along the its circumference. The element type used for structural analysis was 8 node hexahedral reduced integration type element, C3D8R. The isotropic hardening constitutive model was used with the strain rate dependency controlled by Cowper-Symonds rate dependent power law given by (2) [7].

$$\sigma = \sigma_y . \left[1 + \left(\frac{\dot{\varepsilon}}{P} \right)^m \right] \qquad (2)$$

where, σ_y is the quasi-static yield strength, $\dot{\varepsilon}$ is the strain rate, $P=6500s^{-1}$, $m=0.25$ are the strain rate hardening coefficients for the aluminium alloy. The concentrated forces are applied at the nodes of the structure model which were transformed from electromagnetic body forces (Lorentz forces) at the element center in the electromagnetic domain. The tube was fixed at the ends and symmetry boundary conditions were considered on the symmetry planes.

D. Results and discussion

The transient electromagnetic analysis has been performed using the Abaqus/Standard-electromagnetic solver. The total simulation time used was 200 µs and the time step was chosen as 2.5 µs. The electromagnetic body forces at the element center are mapped on to the nodes in the structural model at every incremental time instances. The structural non-linear dynamic analysis is performed using Abaqus/Standard solver. The results of the analysis in terms of radial deformation are compared with experimental results presented by Ping and Feng [7] as shown in Fig.3.
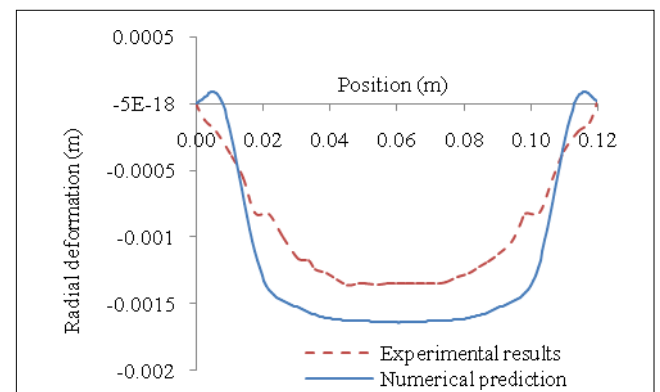

Fig. 3. Comparision of the experimental [7] and numerical results in terms of radial deformation along the position of the tube.

TABLE I.   FREQUENCY AND CORRESPONDING CAPACITANCE, VOLTAGE AT VARIOUS ENERGY LEVELS.

Sr. no.	Capacitance (μF)	Frequency (kHz)	Voltage at different energy levels (kV)					
			1kJ	1.1kJ	1.2kJ	1.3kJ	1.4kJ	1.5kJ
1	60	18.18	5.77E+03	6.06E+03	6.32E+03	6.58E+03	6.83E+03	7.07E+03
2	90	14.84	4.71E+03	4.94E+03	5.16E+03	5.37E+03	5.58E+03	5.77E+03
3	120	12.85	4.08E+03	4.28E+03	4.47E+03	4.65E+03	4.83E+03	5.00E+03
4	240	9.091	2.89E+03	3.03E+03	3.16E+03	3.29E+03	3.42E+03	3.54E+03
5	360	7.352	2.36E+03	2.47E+03	2.58E+03	2.69E+03	2.79E+03	2.89E+03
6	480	6.428	2.04E+03	2.14E+03	2.24E+03	2.33E+03	2.42E+03	2.50E+03
7	600	5.749	1.83E+03	1.91E+03	2.00E+03	2.08E+03	2.16E+03	2.24E+03
8	702	5.315	1.69E+03	1.77E+03	1.85E+03	1.92E+03	2.00E+03	2.07E+03
9	720	5.248	1.67E+03	1.75E+03	1.83E+03	1.90E+03	1.97E+03	2.04E+03
10	840	4.859	1.54E+03	1.62E+03	1.69E+03	1.76E+03	1.83E+03	1.89E+03
11	960	4.545	1.44E+03	1.51E+03	1.58E+03	1.65E+03	1.71E+03	1.77E+03
12	1080	4.285	1.36E+03	1.43E+03	1.49E+03	1.55E+03	1.61E+03	1.67E+03
13	1200	4.065	1.29E+03	1.35E+03	1.41E+03	1.47E+03	1.53E+03	1.58E+03
14	1800	3.319	1.05E+03	1.11E+03	1.15E+03	1.20E+03	1.25E+03	1.29E+03

The numerical results of tube deformation were found to follow the trend of experimental results. The variation in the magnitudes of the deformation from the experimental results is justified by the use of loose coupled approach. In addition the current was assumed to be uniformly distributed across the cross section i.e. the effect of skin depth is neglected.

III.   PARAMETRIC STUDY

The deformation of the tube is controlled by current frequency and discharge energy. A parametric study is performed to investigate the effect of the variation of capacitance and hence the discharge current frequency at different energy levels on the final tube deformation. The voltages are evaluated at various levels of discharge energy and the results are presented in Table 1. This table could be handy in selecting a particular combination of capacitance and voltage value for a given energy level. The coil size was kept constant and the inductance was considered as 1.277μH. The effect of frequency variation on discharge current was investigated by simulating the discharge current at various time and the results are shown in Fig. 4. The energy efficiency is defined as the ratio of final plastic strain energy to the discharge energy. The time variation of discharge energy is given such that:

$$E = E_{ini}.\cos^2\left(\omega t\right).e^{-2\beta t} \qquad (3)$$

where, E is the discharge energy varying with time in joules, E_{ini} is the initial discharge energy in joules, β is the damping coefficient in s^{-1}, ω is the angular frequency in rad/sec.

The variation of discharge energy and plastic strain energy in the tube with time is evaluated at a frequency of 12.85kHz and at a voltage of 4.08kV as shown in Fig.5. The plastic strain energy in the tube increases with its plastic deformation. It reaches its maximum value at the maximum tube deformation and then it oscillates about this value. The plastic strain energies were obtained numerically for each of the combination of capacitance and voltage and the corresponding efficiencies were calculated. It was observed from Fig.6 that for a given energy level the efficiency first increases with the

frequency and then decreases after a certain value. Higher efficiency was obtained between frequency range of 4.859kHz and 5.749kHz for all the energy levels. For instance, the highest efficiency at 1.3kJ was found to be around 13%. Secondly, it was observed that for a given frequency the efficiency increases with increase in the energy level. To sum up, out of all the frequency values and initial discharge energy levels the maximum efficiency was found to be around 16% at frequency 5.315kHz. Thus the EMF process can be optimized for the studied setup at a given energy level. It was also observed that the maximum deformation and hence efficiency was obtained for a slightly lower frequency with increased energy levels. For example, at 1kJ discharge energy the frequency at maximum efficiency was found to be 5.749kHz, whereas the maximum efficiency at 1.5kJ was obtained at 5.315kHz. Thus it can be inferred that the discharge energy has very less impact on the frequency at which maximum deformation is obtained.
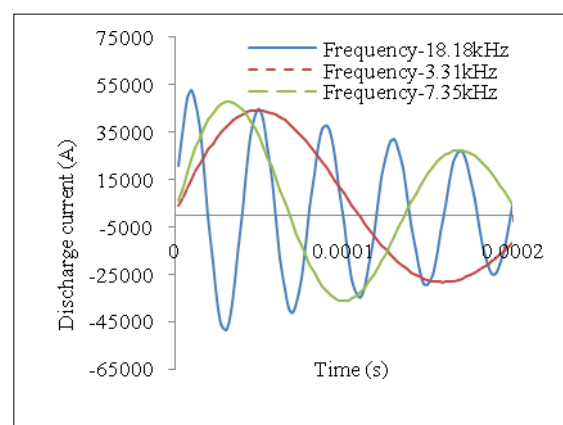

Fig. 4 Variation of discharge current with time at various frequencies.

The variation of maximum velocity at the center of the tube with respect to frequency at different energy levels is plotted in Fig.7. An increasing trend in maximum velocity could be observed at the tube center; however, it decreases after 7.325 kHz. As the energy level is raised, the maximum value of velocity at tube center also increases. Higher energy levels showed higher values of maximum velocities. It was also noticed that the higher values of velocity at the tube center occurred between frequency range 5.315kHz to

9.09kHz at all energy levels. For higher velocity the wrinkling and spring back is reduced; thus the optimum velocity for the current setup was found to be 7.325kHz.
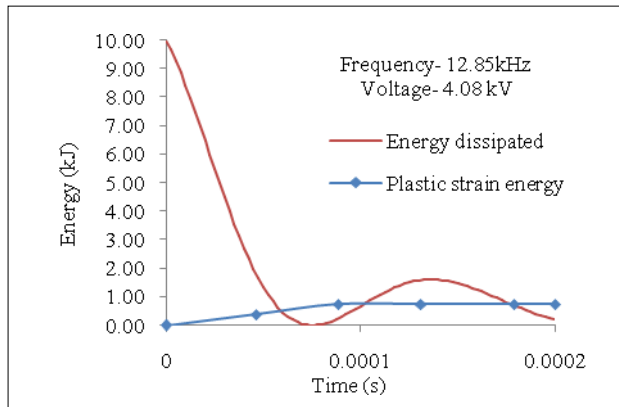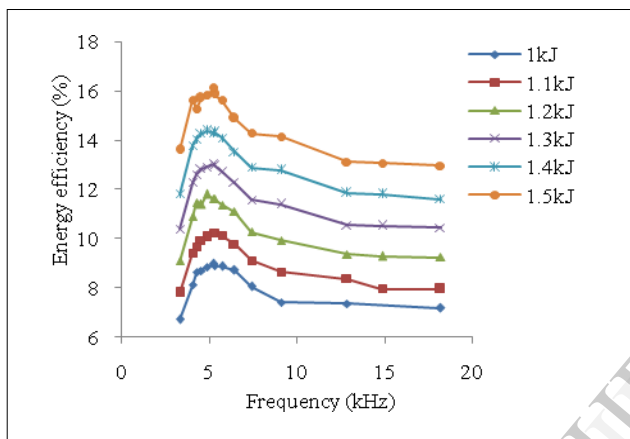

Fig. 5 Variation of energy with time.

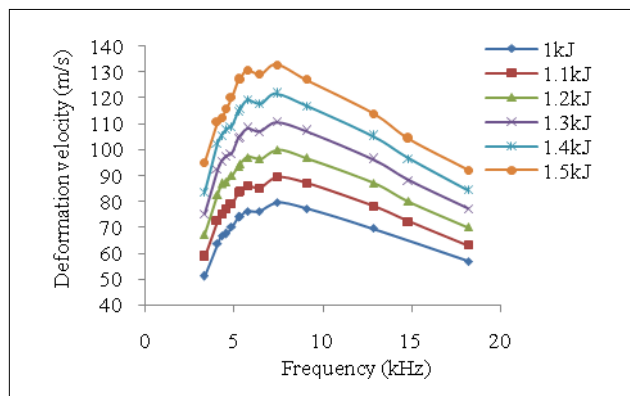Fig. 6 Variation of effeciency with frequency at various energy levels.

Fig. 7 Variation of maximum velocity at tube center with frequency at different energy levels.

IV. CONCLUSION

In this paper numerical simulation of tube compression process is presented using commercially available finite element tool Abaqus®. The final tube deformation was compared with experimental data available in the literature. The numerical results predicted the experimental trend with minor variation in the magnitude between the two which is due to the assumptions made to simplify the numerical analysis. Thus, good correlation is seen between the numerical and the experimental results. Then the parametric study was performed to determine the effect of discharge current frequency and discharge energy on energy efficiency of the system. The energy efficiency was found to be increasing with increasing energy levels for the energy range between 1kJ and 1.5kJ. Higher efficiencies were obtained between the frequency range of 4.859kHz to 5.749kHz. Finally, variations of maximum velocity at center of the tube with frequency at different energy levels were studied and frequency for maximum velocity at tube center was found to be lying between 5.315kHz and 9.091kHz. These high velocities increase the formability and reduce the wrinkling and spring back of the workpiece. This study provides a valuable piece of information for better design of the process.

REFERENCES

[1] Al-Hassani S.T.S, "Magnetic pressure distribution in the sheet metal forming," Electrical methods of machining, forming and coating, Institute of electrical engineering conference, publication no 1975, pp. 1-10.

[2] Jablonski J. and Wrinkler R., "Analysis of electromagnetic forming process," International journal of mechanical sciences, Berlin, vol 20, pp. 315-325, 1978.

[3] Willam H. Gourdin, "Analysis and assessment of electromagnetic ring expansion as a high strain rate test," Journal of applied Physics, California, vol65, pp. 411-422, 1989.

[4] N. Takatsu, M. Kato, K. Sato, T. Tobe, "High speed forming of metal sheet by electromagnetic forces," International journal of Japanese Society for Mechanical Engineering, Japan, vol. 60, pp. 142-148, 1980.

[5] Naveen Kumar, M. Nabi, "Finite Element Modeling and Simulation of Electromagnetic Forces in Electromagnetic Forming Processes: Case Studies using COMSOL Multiphysics," COMSOL users' Conference, Bangalore, India, Nov 2009.

[6] M.A. Siddiqui, J.P.M. Correia, S.Ahzi, S, Belouettar, "Electromagnetic forming process: estimation of magnetic pressure in tube expansion and numerical simulation," Proceedings of the 12th ESAFORM Conference on Material Forming, Netherlands, April 2009.

[7] YU Hai-ping, LI Chun-feng, "Effects of coil length on tube compression in electromagnetic forming," Transactions of Nonferrous Metals Society of China, China, vol. 17, pp. 1270-1275, September 2007.

[8] YU Hai-ping, LI Chun-feng, "Effects of current frequency on electromagnetic tube compression," Journal of materials processing technology, China, vol. 209, pp. 1053-1059, January 2009.

[9] M.A. Siddiqui, "Numerical modeling and simulation of electromagnetic forming process," Thesis, Université de Strasbourg, Europe, June 2009.

[10] M.A.Bahmani, K. Niayesh, A. Karimi, "3D simulation of magnetic field distribution in electromagnetic forming systems with field shaper," Journal of Materials Processing Technology, Tehran, Iran, vol. 209, pp. 2295−2301, March 2009.

[11] Zhang H., Murata M., Suzuki H, "Effects of various working condition on tube bulging by Electromagnetic forming," Journal of Materials Processing Technology, Japan, vol. 48, pp. 113-121, January 1995.